Hyperelectronic Metal−Carborane Analogues of Cymantrene ($MnCp(CO)_3$) Anions: Electronic and Structural Noninnocence of the Tricarbadecaboranyl Ligand

Ayman Nafady,[†,‡] Robert Butterick III,[§] Maria José Calhorda,*[,⊥] Patrick J. Carroll,[§] Daesung Chong,[†] William E. Geiger,*[,†] and Larry G. Sneddon*[,§]

Department of Chemistry, University of Vermont, Burlington Vermont 05405, Department of Chemistry, University of Pennsylvania, Philadelphia, Pennsylvania 19104, and Departamento de Química e Bioquímica, Faculdade de Ciências, Universidade de Lisboa, 1749-016, Lisboa, Portugal

Received May 18, 2007

The reduction of 1,1,1-$(CO)_3$-2-Ph-*closo*-1,2,3,4-$MnC_3B_7H_9$, **1**, to the hyperelectronic dianion $\mathbf{1}^{2-}$ has been studied by electrochemistry, spectroscopy, X-ray crystallography, and DFT calculations. Depending on the medium, this cymantrene derivative displays either a single two-electron wave or two separate one-electron waves in cyclic voltammetry scans, always at potentials (e.g., $E_{1/2} = -1.14$ V vs ferrocene for $\mathbf{1}/\mathbf{1}^-$ in THF) that are very far positive of that reported for $MnCp(CO)_3$ (−2.86 V). Reduction of the corresponding Re compound **2** occurs in a single two-electron process. Both $\mathbf{1}^-$ and $\mathbf{1}^{2-}$ were isolated as their decamethylcobaltocenium salts and characterized by X-ray crystallography. The hapticity of the tricarbadecaboranyl ligand is reduced from hexahapto (η^6) in **1** to tetrahapto (η^4) in $\mathbf{1}^{2-}$, mimicking an η^5/η^3 haptotropic rearrangement of a cyclopentadienyl ligand. The dianion $\mathbf{1}^{2-}$ retains coordination to the C7−B3−B4−C9 face of the tricarbadecaboranyl ligand, much like that found previously for the neutral isocyanide adduct $(CNBu^t)(CO)_3MnC_3B_7H_9$, **3**, showing that the metal−ligand bonding reacts similarly to gain of either two electrons or an electron pair donor. The monoanion $\mathbf{1}^-$ also shows ligand slippage to an η^4 coordination in which relevant distances and angles are roughly intermediate of **1** and $\mathbf{1}^{2-}$. The SOMO of $\mathbf{1}^-$ is highly delocalized over the $Mn-C_3B_7$ framework. Although the tricarbadecaboranyl anion has a strongly electron-accepting ligand effect, the majority of the stabilization energy it imparts to nominally hyperelectronic metals originates from its flexibility in hapticity changes. By analogy to well-documented metal−chelate chemistry, the tricarbadecaboranyl group behaves as a "noninnocent" ligand in these electron-rich systems.

Introduction

Hyperelectronic transition metal complexes function as an important electron source for chemical reactions.[1] Recent work has heightened awareness that electron-rich systems may promote key reduction processes, including those of small molecules and ions.[2] Metal−ligand complexes that can alter their coordination spheres when engaged in single or multiple electron-transfer (e.t.) processes are of particular interest, as shown by activity in the area of reductions of metal arenes.[3−6] These include the important class of "half-sandwich" arene metal carbonyl compounds, which have been shown to undergo interesting structural rearrangements and hydride shifts when reduced to putative 19 e^- or 20 e^- species.[5,6]

Fewer findings have been reported, however, for reduced cyclopentadienyl-type half-sandwich complexes, for which the cathodic chemistry has been dominated by studies of complexes containing the easily slip/folded indenyl ligand.[7] Although the prototypical "piano-stool" complexes $MCp(CO)_3$, M = Mn (cymantrene) or Re, Cp = (C_5H_5), have been calculated to undergo ligand slipping and/or folding to accommodate nominally 20-electron dianionic forms,[8] their cathodic reduction products are not well characterized. Lee and Cooper showed

* Corresponding authors. E-mail: mjc@fc.ul.pt (M.J.C.); william.geiger@uvm.edu (W.E.G.); lsneddon@sas.upenn.edu (L.G.S.).

† University of Vermont.

‡ Present address: School of Chemistry, Monash University, Clayton, Victoria 3800, Australia.

§ University of Pennsylvania.

⊥ Universidade de Lisboa.

(1) For examples see: (a) Geiger, W. E. *Acc. Chem. Res.* **1995**, *28*, 351. (b) Astruc, D. *Electron Transfer and Radical Processes in Transition-Metal Chemistry*; VCH Publishers: New York, 1995; pp 145, 210, 340, 386.

(2) Some leading references are: (a) (CO_2) Appel, A.M.; Newell, R.; Dubois, D. L.; Rakowski DuBois, M. *Inorg. Chem.* **2005**, *44*, 3046. (b) (N_2) Schrock, R. R. *Acc. Chem. Res.* **2005**, *38*, 955. (c) (H_2 evolution) Borg, S. J.; Behrsing, T.; Besp, S. P.; Razavet, M.; Liu, X.; Pickett, C. J. *J. Am. Chem. Soc.* **2004**, *126*, 16988. Also: Felton, G. A. N.; Glass, R. S.; Lichtenberger, D. L.; Evans, D. H. *Inorg. Chem.* **2006**, *45*, 9181. Tye, J. W.; Lee, J.; Wang, H-W.; Mejia-Rodriguez, R.; Reibenspies, J. H.; Hall, M. B.; Darensbourg, M. Y. *Inorg. Chem.* **2005**, *44*, 5550 (d) (Olefin polymerization) Scott, J.; Gambarotta, S.; Korobkov, I. Budzelaar, P. H. M. *Organometallics* **2005**, *24*, 6298.

(3) Ru arenes: (a) Fischer, E. O.; Elschenbroich, C. *Chem. Ber.* **1970**, *103*, 162. (b) Laganis, E. D.; Voegeli, R. H.; Swann, R. T.; Finke, R. G.; Hopf, H.; Boekelheide, V. *Organometallics* **1982**, *1*, 1415. (c) Finke, R. G.; Voegeli, R. H.; Laganis, E. D.; Boekelheide, V. *Organometallics* **1983**, *2*, 347. (d) Pierce, D. T.; Geiger, W. E. *J. Am. Chem. Soc.* **1992**, *114*, 6063.

(4) Rh arenes: (a) Bowyer, W. J.; Geiger, W. E. *J. Am. Chem. Soc.* **1985**, *107*, 5657. (b) Bowyer, W. J.; Merkert, J.; Geiger, W. E.; Rheingold, A. L. *Organometallics* **1989**, *8*, 191. (c) Merkert, J.; Nielson, R. M.; Weaver, M. J.; Geiger, W. E. *J. Am. Chem. Soc.* **1989**, *111*, 7084.

(5) Cr arenes: (a) Rieke, R. D.; Arney, J. S.; Rich, W. E.; Willeford, B. R.; Poliner, B. S. *J. Am. Chem. Soc.* **1975**, *97*, 5951. (b) Rieke, R. D.; Henry, W. P. *J. Am. Chem. Soc.* **1983**, *105*, 6314 (c) Rieke, R. D.; Henry, W. P.; Arney, J. S. *Inorg. Chem.* **1987**, *26*, 420. (d) Leong, V. S.; Cooper, N. J. *J. Am. Chem. Soc.* **1988**, *110*, 2644.

(6) (a) Mn arenes: Veauthier, J. M.; Chow, A.; Fraenkel, G.; Geib, S. J.; Cooper, N. J. *Organometallics* **2000**, *19*, 3942, and references therein. (b) Reingold, J. A.; Rheingold, A. L.; Virkaitis, K. L.; Carpenter, G. B.; Sun, S.; Sweigart, D. A.; Czech, P. T.; Overly, K. R. *J. Am. Chem. Soc.* **2005**, *127*, 11146.

10.1021/om700496v CCC: $37.00
Publication on Web 08/04/2007

that the chemical reduction of $Mn(C_5H_4Me)(CO)_3$ by the alkalide [K(18-crown-6)]K in THF gave an apparent dianion for which an η^3-cyclopentadienyl hapticity was proposed.[9] The electrochemical reduction of the close analogue $MnCp(CO)_3$ is a chemically irreversible one-electron process, however, in THF/$[NBu_4][PF_6]$,[10] and details of the reductive electron-transfer reactions of this series of complexes are still open to inquiry. In this paper we report on the reduction of complexes in which the Cp ligand has been replaced by the behaviorally analogous tricarbadecaboranyl ligand,[11] allowing for characterization and preparation of hyperelectronic anions of both Mn and Re tricarbonyl complexes.

Tricarbadecaboranyl ligands of the type $[6\text{-R-}5,6,9\text{-}C_3B_7H_9]^-$ are well known to exhibit coordination tendencies similar to those of the cyclopentadienyl ligand.[11] We bring attention to the analogy between an η^6 to η^4 haptotropic rearrangement of the $[RC_3B_7H_9]^-$ anion and an η^5 to η^3 rearrangement of the Cp anion, as shown below. Also pertinent to the present work is the strikingly different electron-accepting abilities of the two ligands.[12] Specifically, the tricarbadecaboranyl ligand may function as a "partial electron reservoir", allowing access to hyperelectronic organometallic systems.

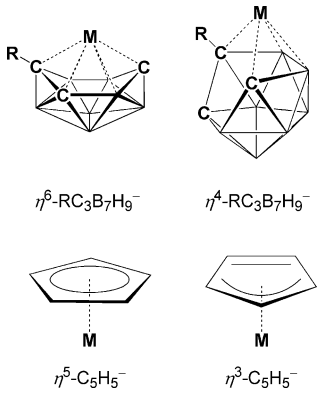

Although 18-electron complexes of the $[C_5H_5]^-$ and $[6\text{-Me-}5,6,9\text{-}C_3B_7H_9]^-$ ligands carry the same charge, lower metal oxidation states are strongly stabilized by the latter, as demonstrated by comparison of $E_{1/2}$ potentials of their analogous complexes. A shift of +0.44 V was reported for a series of Fe and Ru complexes underdoing *oxidation* to 17 e^- systems when a Cp ring was replaced by a tricarbadecaboranyl ligand.[12b] This ligand electronic effect[13] is, in itself, not surprising given the opportunity for increased charge dispersal into the larger tricarbadecaboranyl ligand. Much greater $E_{1/2}$ changes were seen, however, in some cases exceeding +2 V, for *reductions* of these 18 e^- systems, far in excess of the shifts expected by the ligand electronic effect. Focusing on the heavier metals, the one-electron reductions of $M(\eta^6\text{-}MeC_3B_7H_9)_2$ (M = Ru, Os) are more positive than those of their metallocene counterparts by an impressive 2.6 V.[12b] This raised the possibility that the LUMOs of the iron-group $M(\eta^6\text{-}MeC_3B_7H_9)_2$ complexes might be strictly ligand-based (similar to $[Ru(bipy)_3]^{2+/+}$ type or metalloporphyrin systems),[14] or at least highly metal−ligand delocalized. As shown below, it is a combination of a delocalized LUMO and a redox-initiated hapticity change that is responsible for the enormous stabilization of very low formal metal oxidation states in these tricarbadecaboranyl complexes.

In an earlier paper,[12b] we hypothesized that sequences of electron-transfer (e.t.)-induced structural changes might account for the unusual redox behavior of the Ru tricarbadecaboranyl systems. Specifically, an η^6 to η^4 hapticity change of the type known to accompany the thermally driven addition of *tert*-butyl isocyanide to Ru or Fe tricarbadecaboranyl complexes was invoked.[12a] A further example of such a hapticity change has recently been shown to extend to isocyanide adducts of the manganese-group complexes reported in this paper.[15] Being conceptually similar to the often invoked η^5/η^3 haptotropic rearrangements of Cp ligands,[16] the η^6/η^4 rearrangement of the tricarbadecaboranyl ligand gave further strength to the $[C_5H_5]^-/[RC_3B_7H_9]^-$ analogy. It raised the importance of probing the relationship between structure and electron count for an accessible series of electron-rich species in a way that has not proven possible with the Cp analogues.

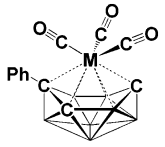

We now report the outcome of a more detailed study on the redox processes of metal−tricarbadecaboranyl complexes, fo-

(7) (a) Pereira, C. C. L.; Costa, P. J.; Calhorda, M. J.; Freire, C.; Rodrigues, S. S.; Herdtweck, E.; Romão, C. C. *Organometallics* **2006**, *25*, 5223. (b) Santi, S.; Broccardo, L. *Organometallics* **2003**, *22*, 3478. (c) Stoll, M. E.; Belanzoni, P.; Calhorda, M. J.; Drew, M. G. B.; Félix, V.; Geiger, W. E.; Gamelas, C. A.; Gonçlaves, I. S.; Romão, C. C.; Veiros, L. F. *J. Am. Chem. Soc.* **2001**, *123*, 10595. (d) Amatore, C.; Ceccon, A.; Santi, S.; Verpeaux, J. N. *Chem.−Eur. J.* **1997**, *3*, 279. (e) Pevear, K. A.; Banaszak Holl, M. M.; Carpenter, G. B.; Rieger, A. L.; Rieger, P. H.; Sweigart, D. A. *Organometallics* **1995**, *14*, 512. (f) Lee, S.; Lovelace, S. R.; Cooper, N. J. *Organometallics* **1995**, *14*, 1974. (g) Miller, G. A.; Therien, M. J.; Trogler, W.C. *J. Organomet. Chem.* **1990**, *383*, 271.

(8) (a) Veiros, L. F. *Organometallics* **2000**, *19*, 5549. (b) Veiros, L. F. *J. Organomet. Chem.* **1999**, *587*, 221. There is, of course, a close conceptual parallel between addition of either two electrons or a two-electron donor to a molecule. For leading references to haptotropic shifts involving the latter see: (c) Basolo, F. *New J. Chem.* **1994**, *18*, 19. (d) Cohen, R.; Weitz, E.; Martin, J. M. L.; Ratner, M. A. *Organometallics* **2004**, *23*, 2315.

(9) Lee, S.; Cooper, N. J. *J. Am. Chem. Soc.* **1991**, *113*, 716.

(10) (a) Sawtelle, S. M.; Johnston, R. F.; Cook, C. C. *Inorg. Chim. Acta* **1994**, *221*, 85 (the reported potential of $E_{pc} = -2.46$ V vs Ag/AgCl in THF/$[NBu_4][BF_4]$ converts to −2.86 V vs ferrocene. (b) The electrochemical reduction of cymantrene has also been reported in acetonitrile (−2.90V vs FcH), and the origin of the chemical irreversibility was examined by spectroscopy: see Salmain, M.; Jaouen, G.; Fiedler, J.; Sokolová, R.; Pospíšil, L. *Collect. Czech. Chem. Commun.* **2001**, *66*, 155.

(11) (a) Plumb, C. A.; Carroll, P. J.; Sneddon, L. G. *Organometallics* **1992**, *11*, 1665. (b) Plumb, C. A.; Carroll, P. J.; Sneddon, L. G. *Organometallics* **1992**, *11*, 1672. (c) Barnum, B. A.; Carroll, P. J.; Sneddon, L. G. *Organometalllics* **1996**, *15*, 645. (d) Weinmann, W.; Wolf, A.; Pritzkow, H.; Siebert, W.; Barnum, B. A.; Carroll, P. J.; Sneddon, L. G. *Organometalllics* **1995**, *14*, 1911. (e) Barnum, B. A.; Carroll, P. J.; Sneddon, L. G. *Inorg. Chem.* **1997**, *36*, 1327. (f) Müller, T.; Kadlecek, D. E.; Carroll, P. J.; Sneddon, L. G.; Siebert, W. J. *Organomet. Chem.* **2000**, *125*, 614−615. (g) Ramachandran, B. M.; Carroll, P. J.; Sneddon, L. G. *Inorg. Chem.* **2004**, *43*, 3467 (h) Ramachandran, B. M.; Carroll, P. J.; Sneddon, L. G. *J. Am. Chem. Soc.* **2000**, *122*, 11033.

(12) (a) Wasczcak, M. D.; Wang, Y.; Garg, A.; Geiger, W. E.; Kang, S. O.; Carroll, P. J.; Sneddon, L. G. *J. Am. Chem. Soc.* **2001**, *123*, 2783. (b) Ramachandran, B. M.; Trupia, S. M.; Geiger, W. E.; Carroll, P. J.; Sneddon, L. G. *Organometallics* **2002**, *21*, 5078.

(13) Lever et al. have compiled electronic effects for a large number of ligands, and leading references may be found in: Lu, S.; Strelets, V. V.; Ryan, M. F.; Pietro, W. J.; Lever, A. B. P. *Inorg. Chem.* ***1996***, *35*, 1013. Compared to the C_5H_5 ligand, the electronic parameters are 0.44 V for $RC_3B_7H_9$, 0.17 V for C_5H_4Br, and −0.27 V for C_5Me_5. Based on the measurements of Hawthorne et al., a value of −0.29 V has been reported (see Geiger, W. E. In *Metal Interactions with Boron Clusters*; Grimes, R. N., Ed.; Plenum Press: New York, 1982; p 239) for the Cp-like dicarbollide ligand $[C_2B_9H_{11}]^{2-}$.

(14) There is a vast literature involving variations on this theme. For early references on $Ru^{II}N_6$ see: Juris, A.; Balzani, V.; Barigelletti, F.; Campagna, S., Belser, P.; von Zelewsky, A. *Coord. Chem. Rev.* **1988**, *84*, 85. On metalloporphyrin systems see: Guilard, R.; Kadish, K. M. *Chem. Rev.* **1988**, *88*, 1121.

cusing here on the reduction of 1,1,1-$(CO)_3$-2-Ph-*closo*-1,2,3,4-$MC_3B_7H_9$, M = Mn, **1**, and Re, **2**. These complexes were chosen both for their analogy to traditional piano-stool complexes and for the promise of utilizing their IR-active carbonyl groups and the ESR-active Mn or Re nuclei in mapping the spin and charge distributions of the anions. Careful manipulation of the solvent/electrolyte medium was required in order to obtain both the monoanion and the dianion of the Mn system. The results draw attention to the role of metal−ligand delocalization in nominally 19 e^- and 20 e^- organometallic systems, which has been detailed in relatively few cases.[1a,17] We conclude that the tricarbaboranyl ligand should be considered a "noninnocent" ligand, a term that has been largely absent from the organometallic literature, but which is widely used in transition metal chelate chemistry to describe a ligand capable of functioning as a flexible electron sink.[18]

Experimental Section

Experiments were carried out under nitrogen.

Reagents. 1,1,1-$(CO)_3$-2-Ph-*closo*-1,2,3,4-$MC_3B_7H_9$, M = Mn, **1**, and Re, **2**, were prepared by literature methods.[15] Acceptable elemental analyses (Robertson Analytical Laboratory) were obtained for new compounds. $CoCp^*_2$ ($Cp^* = \eta^5$-C_5Me_5) was purchased from Strem Chemical Co. The tetraalkylammonium salts of $[B(C_6F_5)_4]^-$ (TFAB) and $[B((CF_3)_2C_6H_3)_4]$ ($BArF_{24}$) were prepared by metathesis of either K[TFAB] or Na[$BArF_{24}$] (both purchased from Boulder Scientific Co., Boulder, CO) with the appropriate $[NR_4]Br$ salt in aqueous solution. A detailed description of the preparation and purification of $[NBu_4]$[TFAB] has appeared.[19] The tetraethylammonium salts of $[TFAB]^-$ and $[BArF_{24}]^-$ were recrystallized from CH_2Cl_2/diethyl ether and vacuum-dried. $[NBu_4][PF_6]$ was prepared by metathesis of $[NBu_4]I$ and $[NH_4][PF_6]$ in hot acetone, recrystallized several times from 95% ethanol, and vacuum-dried at 100 °C. Reagent-grade solvents were first distilled from appropriate drying agents into round-bottom storage flasks that contained either CaH_2 (for dichloromethane and acetonitrile), potassium (for diethyl ether and hexanes), or potassium/benzophenone (THF). When being used in an electrochemical experiment or a chemical reduction, the solvent was transferred to another vessel under static vacuum following extensive freeze−pump−thaw cycles and then introduced into a Vacuum Atmospheres drybox.

$[CoCp^*_2][1,1,1\text{-}(CO)_3\text{-}2\text{-}Ph\text{-}1,2,3,4\text{-}MnC_3B_7H_9^-]$ (1^-). The decamethylcobaltocenium salt of $\mathbf{1}^-$ was prepared by the reaction of equivalent quantitites of **1** and $CoCp^*_2$ in THF. A solution of $CoCp^*_2$ (6.5 mg, 0.0197 mmol) in 1 mL of THF was added slowly to a 1 mL solution of **1** (7.5 mg, 0.022 mmol) in THF and then stirred at 243 K for ca. 10 min, causing a color change from golden yellow to deep orange. Precipitation of $[CoCp^*_2]\mathbf{1}^-$ was achieved by slow addition of dry pentane (5 mL) into the reaction mixture under vigorous stirring for 1 h. The resulting red solid was filtered, washed with pentane (3 × 5 mL), and dried overnight under vacuum. IR spectra of the solid were consistent with those obtained for electrochemically produced $\mathbf{1}^-$. X-ray quality crystals were grown from THF/pentane at 298 K under N_2.

$[CoCp^*_2]_2[8,8,8\text{-}(CO)_3\text{-}9\text{-}Ph\text{-}nido\text{-}8,7,9,10\text{-}MnC_3B_7H_9^{2-}]$ (1^{2-}). The bis-decamethylcobaltocenium salt of $\mathbf{1}^{2-}$ was prepared by the reaction of **1** with 2 equiv of $CoCp^*_2$ in toluene. A solution of $CoCp^*_2$ (13 mg, 0.0394 mmol) in 1.5 mL of toluene was added slowly to a 3 mL solution of **1** (6.67 mg, 0.0197 mmol) in toluene with stirring over ca. 10 min, producing a black solid, which was filtered, washed with toluene (3 × 5 mL), and dried overnight under vacuum. X-ray quality crystals were grown from CH_3CN/diethyl ether at 298 K under N_2.

Electrochemistry. Voltammetry and electrolysis experiments were carried out under standard three-electrode methodologies utilizing a PARC 273A potentiostat in conjunction with homemade software. A fuller description of the procedures employed is available elsewhere.[20] The IR spectroelectrochemistry experiments were carried out under Schlenk conditions, but all other electrochemical procedures and chemical redox reactions were conducted inside the drybox at temperatures controlled by a cooling bath. Voltammetry scans were recorded using a glassy carbon working electrode disk of either 1 or 1.5 mm diameter (Bioanalytical Systems and Cypress Systems, respectively) or a 1.6 mm gold disk (Bioanalytical Systems). The electrodes were pretreated using a standard sequence of polishing with diamond paste (Buehler) of decreasing sizes (3 to 0.25 μm), interspersed by washings with Nanopure water, and finally vacuum drying. The working electrode for bulk electrolyses was a basket-shaped platinum gauze. Analyte concentrations were generally in the range 0.5 to 2 mM.

All potentials in this paper are referred to the ferrocene/ferrocenium reference couple.[21] The potentials were obtained by direct measurement of *in situ* ferrocene added at an appropriate time in the experiment. The experimental reference electrode was Ag/AgCl, separated from solution by a fine frit. A full mechanistic analysis was carried out for each of the observed redox processes using procedures detailed elsewhere.[22] Chemical reversibility on the cyclic voltammetry (CV) time scale was observed for each redox process. Digital simulations were performed using Digisim 3.0 (Bioanalytical Systems).

Spectroscopy. IR spectra were recorded with an ATI-Mattson Infinity Series FTIR interfaced to a computer employing Winfirst software at a resolution of 4 cm^{-1}, and ESR spectra were obtained on a Bruker ESP 300E spectrometer. IR spectroelectrochemistry was performed using a mid-IR fiber-optic "dip" probe (Remspec, Inc), as described in the literature.[20a,23]

Crystallographic Data. Single crystals of compounds $\mathbf{1}^-$ and $\mathbf{1}^{2-}$ were obtained as described above.

Collection and Reduction of the Data. Crystallographic data and structure refinement information are summarized in Table 1. X-ray intensity data for $[CoCp^*_2]\mathbf{1}^-$ (Penn3223) and $[CoCp^*_2]_2\mathbf{1}^{2-}$ (Penn3218) were collected on a Mercury CCD area detector employing graphite-monochromated Mo Kα radiation ($\lambda = 0.71069$ Å). Indexing was performed from a series of 12 0.5°

(15) Butterick, R., III; Ramachandran, B. M.; Carroll, P. J.; Sneddon, L. G. *J. Am. Chem. Soc.* **2006**, *128*, 8626.

(16) Leading references to the haptotropic rearrangement of the Cp ligand: (a) Basolo, F. *Polyhedron* **1990**, *9*, 1503. (b) O'Connor, J. M.; Casey, C. P. *Chem. Rev.* **1987**, *87*, 307. (c) Calhorda, M. J.; Gamelas, C. A.; Romão, C.C.; Veiros, L. F. *Eur. J. Inorg. Chem.* **2000**, 331.

(17) (a) Tyler, D. R. In *Organometallic Radical Processes*; Trogler, W. C., Ed.; Elsevier: Amsterdam, 1990; pp 338 ff. (b) For a systematic set of calculations see the series by Braden, D. A.; Tyler, D. R. in: (i) *Organometallics* **2000**, *19*, 3762; (ii) *Organometallics* **2000**, *19*, 1175; (iii) *Organometallics* **1998**, *17*, 4060; and (iv) *J. Am. Chem. Soc.* **1998**, *120*, 942.

(18) (a) McCleverty, J. A. In *Progress in Inorganic Chemistry*; Cotton, F. A., Ed.; John Wiley and Sons, New York, 1968; Vol. 10, pp 49−219. (b) Mueller-Westerhoff, U. T.; Vance, B. In *Comprehensive Coordination Chemistry*; Wilkinson, G., Gillard, R. D., McCleverty, J., Eds.; Pergamon Press: Oxford, 1987, Vol. 2, pp 595−631. (c) Clemenson, P. I. *Coord. Chem. Rev.* **1990**, *106*, 171. (d) Lim, B. S.; Fomitchev, D. V.; Holm, R. H. *Inorg. Chem.* **2001**, *40*, 4257. (e) Pierpont, C. G.; Lange, C. W. *Prog. Inorg. Chem.* **1994**, *41*, 331. (f) Hirao, T. *Coord. Chem. Rev.* **2002**, *226*, 81 (g) Kaim, W. *J. Chem. Soc., Dalton Trans.* **2003**, 761. (h) Dei, A.; Gatteschi, D.; Sangregorio, C.; Sorace, L. *Acc. Chem. Res.* **2004**, *37*, 827. (i) Chlopek, K.; Bill, E.; Weyhermuller, T.; Wieghardt, K. *Inorg. Chem.* **2005**, *44*, 7087.

(19) LeSuer, R. J.; Buttolph, C.; Geiger, W. E. *Anal. Chem.* **2004**, *76*, 6395.

(20) (a) Shaw, M. J.; Geiger, W. E. *Organometallics* **1996**, *15*, 13. (b) Stoll, M. E.; Lovelace, S. R.; Geiger, W. E.; Schimanke, H.; Hyla-Kryspin, I.; Gleiter, R. *J. Am. Chem. Soc.* **1999**, *121*, 9343.

(21) (a) Gritzner, G.; Kuta, J. *Pure Appl. Chem.* **1984**, *56*, 461. (b) Connelly, N. G.; Geiger, W. E. *Chem. Rev.* **1996**, *96*, 877.

(22) Geiger, W. E. In *Laboratory Techniques in Electroanalytical Chemistry*, 2nd ed.; Kissinger, P. T., Heineman, W. R., Ed.; Marcel Dekker, Inc.: New York, 1996; pp 683 ff.

(23) Stoll, M. E.; Geiger, W. E. *Organometallics* **2004**, *23*, 5818.

Table 1. Crystallographic Data Collection and Structure Refinement Information

	$[Cp^*_2Co]$ $\mathbf{1}^-$	$[Cp^*_2Co]_2$ $\mathbf{1}^{2-}$ (CH_3CN)
empirical formula	$C_{32}B_7H_{44}O_3CoMn$	$C_{54}B_7H_{77}NO_3Co_2Mn$
fw	666.21	1036.64
cryst class	orthorhombic	monoclinic
space group	*Pbca* (#61)	$P2_1/n$ (#14)
Z	8	4
a, Å	14.1426(5)	9.7900(4)
b, Å	17.8443(7)	19.3682(5)
c, Å	26.8185(10)	28.0317(10)
α, deg		
β, deg		91.5988(2)
γ, deg		
V, Å^3	6768.0(4)	5313.2(3)
D_{calc}, g/cm^3	1.308	1.296
μ, cm^{-1}	8.95	8.94
λ, Å (Mo Kα)	0.71069	0.71069
cryst size, mm	0.30 × 0.28 × 0.15	0.40 × 0.36 × 0.20
F(000)	2776	2184
2θ angle, deg	5.48−54.96	5.12−54.96
temperature, K	143	143
hkl collected	$-18 \le h \le 17$, $-22 \le k \le 23$, $-28 \le l \le 34$	$-12 \le h \le 12$, $-20 \le k \le 25$, $-36 \le l \le 34$
no. of reflns measd	41 241	37 152
no. of unique reflns	7697 (R_{int} = 0.0302)	19 152 (R_{int} = 0.0216)
no. of obsd reflns	6252 ($F > 4\sigma$)	10 615 ($F > 4\sigma$)
no. of reflns used in refinement	7697	11 952
no. of params	463	670
R^a indices ($F > 4\sigma$)	$R_1 = 0.0445$ $wR_2 = 0.0975$	$R_1 = 0.0339$ $wR_2 = 0.0813$
R^a indices (all data)	$R_1 = 0.0589$ $wR_2 = 0.1054$	$R_1 = 0.0398$ $wR_2 = 0.0851$
GOF^b	1.091	1.043
final diff peaks, e/Å^3	+0.415, −0.354	+0.632, −0.262

^{a} $R_1 = \sum||F_o| - |F_c||/\sum|F_o|$; $wR_2 = \{\sum w(F_o^2 - F_c^2)^2/\sum w(F_o^2)^2\}^{1/2}$. ^{b} GOF $= \{\sum w(F_o^2 - F_c^2)^2/(n - p)\}^{1/2}$ where n = no. of reflns; p = no. of params refined.

rotation images with exposures of 30 s and a 36 mm crystal-to-detector distance. Oscillation images were processed using CrystalClear,[24] producing a list of unaveraged F^2 and $\sigma(F^2)$ values, which were then passed to the CrystalStructure[25] program package for further processing and structure solution on a Dell Pentium III computer. The intensity data were corrected for Lorentz and polarization effects and for absorption.

Solution and Refinement of the Structures. The structures were solved by direct methods (SIR97[26]). Refinement was by full-matrix least-squares based on F^2 using SHELXL-97.27 All reflections were used during refinement (values of F^2 that were experimentally negative were replaced with $F^2 = 0$).

DFT Calculations. All density functional theory calculations[28] were performed using the Amsterdam Density Functional program package (ADF).[29] Gradient-corrected geometry optimizations,[30] without symmetry constraints, were performed using the local density approximation of the correlation energy (Vosko−Wilk−Nusair),[31] augmented by the exchange−correlation functionals of Perdew−Wang.[32] Relativistic effects were treated with the ZORA approximation.[33] The core orbitals were frozen for Mn ([1−2]s, 2p) and C, B, and O (1s). Triple-ζ Slater-type orbitals (STO) augmented by a set of two polarization functions were used to describe the valence shells of C, B, O, H, and Mn. Unrestricted calculations were performed for the paramagnetic complexes. The carborane ligand was modeled by [6-Me-5,6,9-$C_3B_7H_9$]$^-$. Structures were taken from this work for the anionic complexes and from ref 15 for the neutral species. For the EPR calculations, the *A* values were obtained from an unrestricted calculation and the *g* values from a spin-restricted calculation with spin−orbit correction (ZORA[33]). All-electron basis sets, consisting of uncontracted triple-ζ STO functions, augmented by polarization functions as described above, were used for all elements. The ZORA method[33] was used to account for relativistic effects and the spin−orbit coupling. Graphical representations of molecular orbitals were drawn with MOLEKEL (Lüthi, H. P.; Portmamn, S. *Chimia* **2000**, *54*, 766), and structures and the spin density with Chemcrafts.

Results

I. Electrochemistry. The cathodic process for the manganese compound **1** consists of either a single two-electron wave or two separate one-electron waves, depending on the solvent/supporting electrolyte medium, with $E_{1/2}$ values in the range −1.04 to −1.42 V vs ferrocene. The medium was manipulated to favor or disfavor discrete one-electron processes using recently detailed principles.[34] In the present context involving neutral starting materials and anionic products, the strongest factors favoring discrete one-electron processes (i.e, enlarging the separation in $\Delta E_{1/2}$ values) are the use of relatively nonpolar solvents having strong donor properties and supporting electrolytes having weakly ion-pairing cations.[34]

I.A. From a Two-Electron Process $\mathbf{1 \rightleftharpoons 1^{2-}}$ in $\mathbf{CH_2Cl_2}$ to Separate $\mathbf{1 \rightleftharpoons 1^-}$ and $\mathbf{1^- \rightleftharpoons 1^{2-}}$ Processes in THF. One chemically reversible two-electron reduction wave was observed for **1** in the low-donor solvent dichloromethane. With $[NEt_4]^+$ as the electrolyte cation, well-shaped single-wave voltammograms were observed with characteristics that were difficult to distinguish from those of a quasi-Nernstian one-electron process. For example, a ΔE_p value of 79 mV was observed in slow CV scans and a width at half-height of 89 mV was measured in differential pulse voltammetry scans employing a 10 mV pulse height (for CV, see Figure 1a). The reaction was shown to be a chemically reversible *two*-electron process, however, by bulk cathodic electrolysis, which gave 2 F/equiv. The dianion formed in this process was quantitatively oxidized back to the neutral starting material (also using 2 F/equiv) by anodic re-electrolysis. Linear scan voltammograms taken during the cathodic electrolysis show the smooth conversion to $\mathbf{1}^-$ and then $\mathbf{1}^{2-}$ (Supporting Information Figure S1).

Replacement of $[NEt_4]^+$ by the less ion-pairing $[NBu_4]^+$ resulted in a small but discernible distortion of this wave and the first visual hint of the presence of two closely spaced one-electron processes (Figure 1b). Changing to the stronger donor solvent acetonitrile (DN = 14.1) gave partial separation of the

(24) *CrystalClear*; Rigaku Corporation, 1999.
(25) *CrystalStructure*, Crystal Structure Analysis Package; Rigaku Corp.: Rigaku/MSC, 2002.
(26) *SIR97*: Altomare, A.; Burla, M. C.; Camalli, M.; Cascarano, G. L.; Giovanni, M.; Giacovazzo, C.; Guagliardi, A.; Moliterni, A.; Polidori, G. J.; Spagna, R. *J. Appl. Crystallogr.* **1999**, *32*, 115.
(27) Sheldrick, G. M. *SHELXL-97*, Program for the Refinement of Crystal Structures; University of Göttingen: Germany, 1997.
(28) Parr, R. G.; Young, W. *Density Functional Theory of Atoms and Molecules*; Oxford University Press: New York, 1989.
(29) (a) Te Velde, G.; Bickelhaupt, F. M.; Baerends, E. J.; Fonseca Guerra, C.; Van Gisbergen, S. T. A.; Snijders, J. G.; Ziegler, T. *J. Comput. Chem.* **2001**, *22*, 931. (b) Guerra, C. F.; Snijders, J. G.; Te Velde, G.; Baerends, E. J. *Theor. Chem. Acc.* **1998**, *99*, 391. (c) *ADF2005.01*, SCM, Theoretical Chemistry, Vrije Universiteit: Amsterdam, The Netherlands, http://www.scm.com.
(30) (a) Versluis, L.; Ziegler, T. *J. Chem. Phys.* **1988**, *88*, 322. (b) Fan, L.; Ziegler, T. *J. Chem. Phys.* **1991**, *95*, 7401.
(31) Vosko, S. H.; Wilk, L.; Nusair, M. *Can. J. Phys.* **1980**, *58*, 1200.
(32) Perdew, J. P.; Chevary, J. A.; Vosko, S. H.; Jackson, K. A.; Pederson, M. R.; Singh, D. J.; Fiolhais, C. *Phys. Rev.* **1992**, *B46*, 6671.
(33) van Lenthe, E.; Ehlers, A.; Baerends, E. J. *J. Chem. Phys.* **1999**, *110*, 8943.
(34) Barriere, F.; Geiger, W. E. *J. Am. Chem. Soc.* **2006**, *128*, 3890.

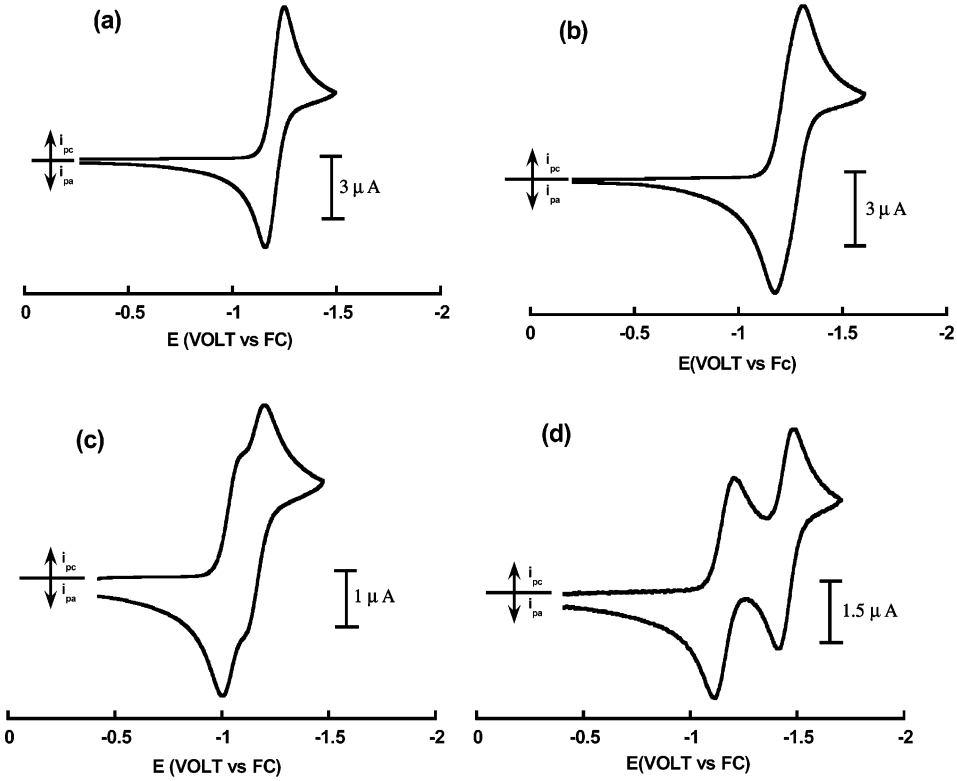

Figure 1. CV scans of **1** at $\nu = 0.1$ V s^{-1} under different conditions: (a) 1.5 mM **1** in CH_2Cl_2/0.1 M $[NEt_4][B(C_6H_3(CF_3)_2)_4]$, GC disk ($d = 1$ mm); (b) 1.0 mM **1** in CH_2Cl_2/0.05 M $[NBu_4]$[TFAB], GC disk ($d = 1$ mm); (c) 0.7 mM **1** in CH_3CN/0.1 M $[NBu_4]$[TFAB], GC disk ($d = 1$ mm); (d) 0.5 mM **1** in THF/0.15 M $[NBu_4][PF_6]$, Au disk ($d = 1.6$ mm).

Table 2. $E_{1/2}$ Values vs Ferrocene/Ferrocenium for 1,1,1-$(CO)_3$-2-Ph-*closo*-1,2,3,4-$MnC_3B_7H_9$ (1) and 1,1,1-$(CO)_3$-2-Ph-*closo*-1,2,3,4-$ReC_3B_7H_9$ (2) under Different Medium Conditions[a]

cmpd	solvent−electrolyte	$E_{1/2}(1)$ (V)	$E_{1/2}(1)$ (V)	$\Delta E_{1/2}$ (mV)	log K_{comp}
1	THF−$[NBu_4][PF_6]$	−1.140	−1.440	300	5.08
1	THF−$[NBu_4][B(C_6F_5)_4]$	−1.180	−1.430	250	4.23
1	THF−$[NBu_4][B(C_6H_3(CF_3)_2)_4]$	−1.181	−1.416	235	3.98
1	THF−$[NEt_4][B(C_6H_3(CF_3)_2)_4]$	−1.185	−1.379	194	3.28
1	MeCN−$[NBu_4][B(C_6F_5)_4]$	−1.040	−1.150	110	1.86
1	CH_2Cl_2−$[NBu_4][B(C_6F_5)_4]$	−1.225	−1.300	75	1.27
1	CH_2Cl_2−$[NEt_4][B(C_6H_3(CF_3)_2)_4]$	−1.222	−1.257	35	0.59
2	THF−$[NBu_4][B(C_6F_5)_4]$	−1.33	−1.27	−60	−1.02

[a] Comproportionation constants for the reactions $\mathbf{1} + \mathbf{1}^{2-} \rightleftharpoons 2\ \mathbf{1}^{-}$ and $\mathbf{2} + \mathbf{2}^{2-} \rightleftharpoons 2\ \mathbf{2}^{-}$ are also given.

two waves (Figure 1c). Finally, voltammetry in THF (DN = 20) exhibits maximally separated waves differing by up to 300 mV(Figure 1d), depending on the supporting electrolyte. The two one-electron redox processes are given in eqs 1 and 2. The

$$Mn(CO)_3(Ph{-}C_3B_7H_9) + e^- \rightleftharpoons [Mn(CO)_3(Ph{-}C_3B_7H_9)]^- \quad E_{1/2}(1), k_s(1) \quad (1)$$

$$[Mn(CO)_3(Ph{-}C_3B_7H_9)]^- + e^- \rightleftharpoons [Mn(CO)_3(Ph{-}C_3B_7H_9)]^{2-} \quad E_{1/2}(2), k_s(2) \quad (2)$$

values of $E_{1/2}$, $\Delta E_{1/2}$ ($= E_{1/2}(1) - E_{1/2}(2)$), and the equilibrium constants based on the comproportionation reaction of eq 3 are collected in Table 2. The $\Delta E_{1/2}$ values varied from a low of 35 mV in CH_2Cl_2/$[NEt_4][BArF_{24}]$[35] to a high of 300 mV in THF/$[NBu_4][PF_6]$, reflecting an increase of over 10^4 in K_{comp}.[36] The changes follow those predicted by the recently described[34] "mirror image" model of electrolyte influence on $\Delta E_{1/2}$ values. They aid the design of experiments that allow identification (and, in the present case, isolation) of both the one-electron and two-electron reduction products of **1**. Medium effects were not found for "crossover" of the $E_{1/2}$ potentials[37] in which $E_{1/2}(2) > E_{1/2}(1)$.

$$Mn(CO)_3(Ph{-}C_3B_7H_9) + [Mn(CO)_3(Ph{-}C_3B_7H_9)]^{2-} \rightleftharpoons 2\,[Mn(CO)_3(Ph{-}C_3B_7H_9)]^- \quad (3)$$

(35) The potential separation of two unresolved but closely spaced one-electron waves may be obtained by analysis of the ΔE_p separation in cyclic voltammetry or the width at half-height, $W_{1/2}$, in differential pulse voltammograms. Account must be taken of ohmic effects, which in the present case were subtracted by making measurements of a ferrocene standard displaying the same currents as the analyte. The resistance-corrected $W_{1/2}$ value for **1** was 89 mV in CH_2Cl_2/0.1 M $[NEt_4][B(C_6H_3(CF_3)_2)_4]$, allowing the assignment of $E_{1/2}(1) - E_{1/2}(2)$ as 35 mV based on the tabular data in ref 48.

(36) log $K_{comp} = 16.9\Delta E_{1/2}$ at 298 K ($\Delta E_{1/2}$ in V).

(37) (a) Evans, D. H.; Lehmann, M. W. *Acta Chem. Scand.* **1999**, *53*, 765. (b) Macias-Ruvalcaba, N. A.; Evans, D. H. *J. Phys. Chem. B* **2006**, *110*, 5155.

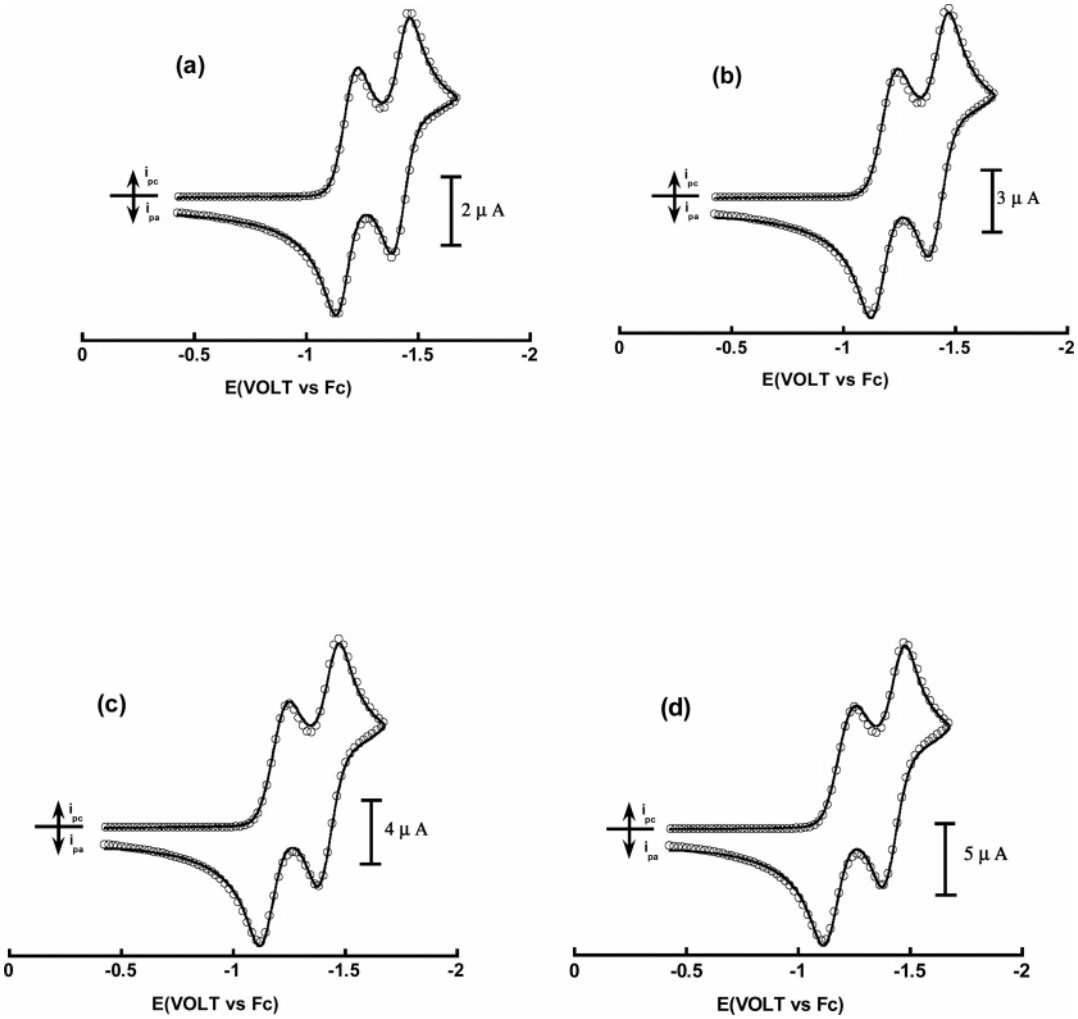

Figure 2. Experimental (solid line) and simulated (circles) background-subtracted CV scans of 0.61 mM **1** in THF/0.1 M [NBu_4][TFAB] at 1.5 mm diameter GC electrode and scan rates of (a) 0.2 V s^{-1}; (b) 0.5 V s^{-1}; (c) 0.75 V s^{-1}; and (d) 1 V s^{-1}. Relevant simulation parameters: $E_{1/2}(1) = -1.18$ V, $E_{1/2}(2) = -1.425$ V; $\alpha_1 = \alpha_2 = 0.5$; $k_s(1) = 0.0088$ cm s^{-1}; $k_s(2) = 0.020$ cm s^{-1}; $D_o = 1.05 \times 10^{-5}$ cm s^{-1}; electrode area = 0.018 cm^2.

I.B. Heterogeneous Electron-Transfer Rates. Given the expectation of structural changes that might accompany these electron-transfer reactions[12b] and the possibility of using an inner-sphere reorganizational model[38] to account for the energies of those changes, the standard heterogeneous electron-transfer rate constants (k_s) were determined for both **1**/**1**$^-$ and **1**$^-$/**1**$^{2-}$ in THF/[NBu_4][TFAB]. The fact that both electron-transfer processes are rather sluggish allowed us to employ modest CV scan rates (0.1 to 2 V s^{-1}) for these measurements. Background-subtracted CV scans obtained under positive-feedback *iR* compensation were of sufficient quality to give k_s values based on the traditional working curves of Nicholson.[39] Higher precision in the k_s determinations was obtained through digital simulations (some of which are shown in Figure 2), yielding $k_s(1)$ (0.0088 ± 0.0007 cm s^{-1}) and $k_s(2)$ (0.020 ± 0.002). In both cases the transfer coefficient, α, appeared to be close to 0.5. A diffusion coefficient of 1.05×10^{-5} cm^2 s^{-1} was measured by chronoamperometry in THF and used in the calculation of the k_s values, the significance of which will be discussed below. Consistent with the lower value of $k_s(1)$, square-wave voltammetry showed a small lowering of the current height of the first reduction compared to the second (Figure S2, Supporting Information).

I.C. Spectroscopic Characterization of Anions. IR spectra were obtained for **1**, **1**$^-$, and **1**$^{2-}$ in both the carbonyl and B−H stretching regions. The shifts in IR bands are consistent with the observed changes in the crystallographically confirmed structures and computational results (*vide infra*). IR spectra of the *dianion* **1**$^{2-}$ were recorded either after a two-electron electrochemical reduction of **1** in CH_3CN at $E_{appl} = -1.8$ V, by monitoring the spectral changes with a fiber-optic absorption probe,[20] or by a chemical reduction followed by routine sampling. For the latter, a solution of **1** in benzene was treated with 2 equiv of $CoCp^*_2$, resulting in precipitation of the dianion. After evaporation of the benzene, the solid was dissolved in CH_3CN to obtain the IR of the dianion. In both cases the three carbonyl features expected for **1**$^{2-}$ were observed as a single absorption band at 1920 ± 1 cm^{-1} and a pair of incompletely resolved bands at approximately 1815 and 1801 cm^{-1} (Figure 3). Compared to neutral **1**, the three ν_{CO} bands are shifted by an average of 167 cm^{-1} to lower energy. Carbonyl-range spectra of the *monoanion* **1**$^-$ were obtained by partial electrolysis of **1** in CH_3CN at $E_{appl} = -1.10$ V. As shown in Figure 3, the three bands for the neutral complex are replaced by a sharp band at 1973 cm^{-1} and a broad absorption at 1893 cm^{-1}, which must contain the other two ν_{CO} bands of **1**$^-$. In this case, the weighted

(38) (a) Marcus, R. A. *J. Chem. Phys.* **1965**, *43*, 679. (b) Hale, J. M. In Hush, N. S., Ed. *Reactions of Molecules at Electrodes*; Wiley-Interscience: London, 1971; pp 229 ff.

(39) Nicholson, R. S. *Anal. Chem.* **1966**, *38*, 1406.

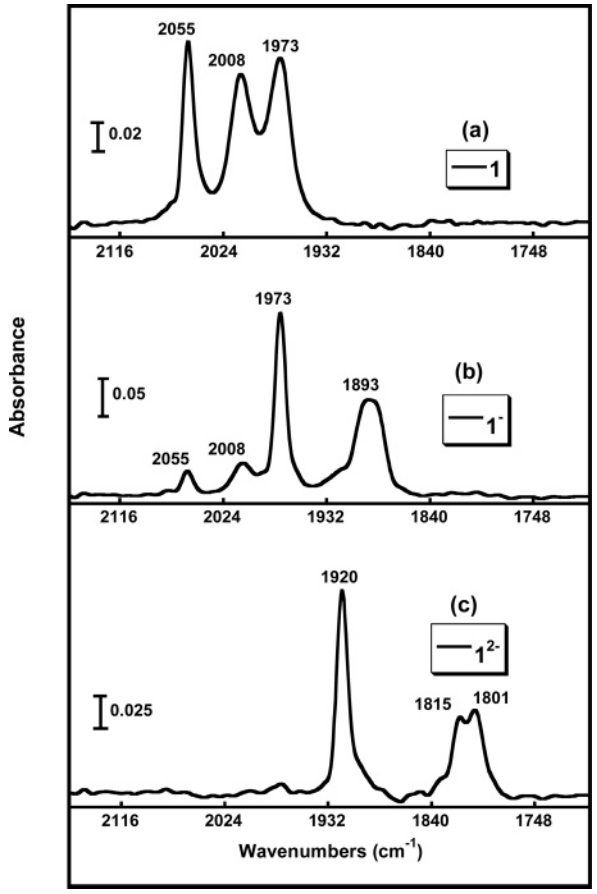

Figure 3. *In situ* IR spectroelectrochemical monitoring of ν_{CO} region during bulk reduction of 1 mM **1** in CH_3CN/0.15 M $[NBu_4][PF_6]$ at 273 K, $E_{appl} = -1.5$ V vs Fc/Fc^+: (a) before bulk electrolysis; (b) after uptake of ca. 1 F/equiv; (c) after uptake of ca. 2 F/equiv.

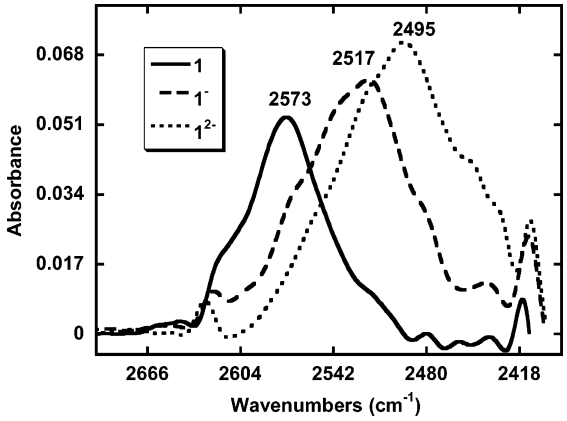

Figure 4. *Ex situ* IR spectra in ν_{BH} region of 1.15 mM **1** in CH_3CN/0.1 M $[NBu_4][PF_6]$ at 298 K, before bulk electrolysis (black curve); after uptake of 0.9 F/equiv at $E_{appl} = -1.1$ V Fc/Fc^+ (red curve); and after uptake of 1.8 F/equiv at $E_{appl} = -1.4$ V vs Fc/Fc^+ (blue curve).

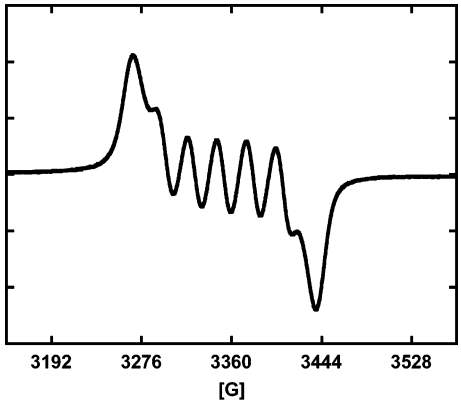

Figure 5. Fluid solution ESR spectra of $\mathbf{1}^-$ generated by chemical reduction of **1** with 1 equiv of $CoCp^*_2$ in THF at 298 K. The microwave frequency was 9.4746 GHz.

average shift to lower field is 95 cm^{-1} compared to the neutral complex. This assignment was confirmed by the chemical reduction of **1** by 1 equiv of $CoCp_2^*$ in THF, which gave a well-shaped symmetric ν_{CO} band at 1972 cm^{-1} and an asymmetric feature at about 1895 cm^{-1}. While clearly consistent with a substantial increase in electron density at the metal center, the redox-induced shifts in ν_{CO} will be discussed more extensively below.

IR spectroscopy was also used to monitor the change in B−H stretching frequencies as a function of the redox state of **1**. In this case, the spectra were obtained by removing samples after bulk electrolysis of **1** in CH_3CN to either the monoanion or dianion. Although the ν_{BH} absorptions of carboranes (2800 to 2350 cm^{-1})[40] are generally complex owing to overlap of a number of B−H fundamentals, they are known to exhibit shifts to lower field with an increase in the negative charge of the carborane.[41] Consider the spectra recorded for **1** and its reduction products (Figure 4). Indeed, a gradual shift to lower frequency occurs upon reduction, with the maximum absorption intensity moving a *total* of −78 cm^{-1} on going from **1** to $\mathbf{1}^{2-}$. We note, however, that this shift is not as large as expected.[42] Furthermore, there is a substantial broadening of the ν_{BH} absorptions in the anions, compared to **1**. A width-at-half-height of approximately 90−95 cm^{-1} is seen for $\mathbf{1}^{2-}$ or $\mathbf{1}^-$, compared to only 55 cm^{-1} for **1**. The likely source of this difference is in the nature of the metal−boron bonding in these systems. As shown below, the Mn atom is bonded to three boron atoms in **1**, but to only two boron atoms in $\mathbf{1}^-$ and $\mathbf{1}^{2-}$. This has the qualitative effect of increasing the number of boron atoms having substantially different electronic properties in the more reduced forms, possibly leading to broadening of the ν_{BH} absorption. Future work on more metallocarboranes undergoing confirmed changes in metal−boron bonding is necessary to test this interpretation.

The monoanion $\mathbf{1}^-$ prepared by either chemical or electrochemical reduction gives an intense ESR spectrum in both fluid and glassy THF. The room-temperature fluid spectrum (Figure 5, $\langle g \rangle = 2.019$) consisted of seven partially resolved lines within a range of roughly 25 G. The peak-to-peak linewidths of ca. 13 G broadened even more at lower fluid temperatures. DFT calculations (*vide infra*) predict that the largest hyperfine splitting (hfs) is from a single boron atom (^{10}B, $I = 3$; ^{11}B, $I = 3/2$) and that additional splittings of about half the value of the boron hfs are expected for ^{55}Mn ($I = 5/2$) and ^1H ($I = 1/2$). If fully resolved, a minimum[43] of 48 lines is therefore predicted, far in excess of the number observed in the fairly broad-lined experimental spectrum. Our attempts to simulate the spectrum, while incomplete, led us to conclude that (i) the fluid spectrum

(40) Leites, L. A. *Chem. Rev.* **1992**, *92*, 279.

(41) Chin, T. T.; Lovelace, S. R.; Geiger, W. E.; Davis, C. M.; Grimes, R. N. *J. Am. Chem. Soc.* **1994**, *116*, 9359.

(42) Corresponding shifts of ±58 to 73 cm^{-1} were measured for one-electron redox reactions involving half-sandwich metal complexes of the $Et_2C_2B_4H_4$ ligand in ref 41.

(43) Additionally, two other smaller hfs also predicted for other nonequivalent borons.

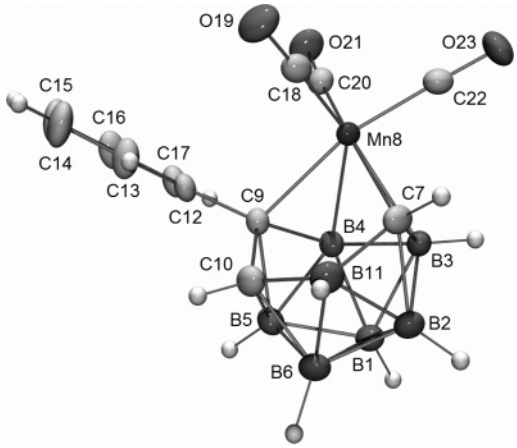

Figure 6. ORTEP representation of 8,8,8-$(CO)_3$-9-Ph-*nido*-8,7,9,-10-$MnC_3B_7H_9^{2-}$ (**1**$^{2-}$). For selected distances see Table 3. Selected angles (deg): C7−Mn8−C9, 83.0(1); Mn8−C9−C12, 114.2(1); C9−Mn8−C18, 92.8(1); C9−Mn8−C20, 96.6(1); C9−Mn8−C22, 165.5(1); C7−Mn8−C18, 95.0(1); C7−Mn8−C20, 168.4(1); C7−Mn8−C22, 90.6(1); Mn8−C18−O19, 178.2(2); Mn8−C20−O21, 176.9(2); Mn8−C22−O23, 178.4(2).

must contain both Mn and B hfs and (ii) there are at least two nuclei having splittings that are an integral multiple of each other, based on the observation of an odd number of lines. We thus leave the specifics of the electron distribution in the SOMO of **1**$^-$ to the DFT calculations, discussed below.

II. Chemical Reduction of 1. Depending on reaction stoichiometry and solvent, reaction of **1** with the reducing agent $CoCp^*_2$ gave the **1**$^-$ or **1**$^{2-}$ anion. If the reaction was carried out in CH_2Cl_2 or toluene with 2 equiv of $CoCp^*_2$, the **1**$^{2-}$ dianion was formed (eq 4).

$$1,1,1\text{-}(CO)_3\text{-}2\text{-Ph-}closo\text{-}1,2,3,4\text{-}MnC_3B_7H_9\ (\mathbf{1}) + 2\ CoCp^*_2 \rightarrow [CoCp^*_2]_2[8,8,8\text{-}(CO)_3\text{-}9\text{-Ph-}nido\text{-}8,7,9,10\text{-}MnC_3B_7H_9]\ (\mathbf{1}^{2-}) \quad (4)$$

If the reaction was performed in THF with 1 equiv of $CoCp^*_2$, **1**$^-$ was produced (eq 5).

$$1,1,1\text{-}(CO)_3\text{-}2\text{-Ph-}closo\text{-}1,2,3,4\text{-}MnC_3B_7H_9\ (\mathbf{1}) + CoCp^*_2 \xrightarrow{THF} [CoCp^*_2][1,1,1\text{-}(CO)_3\text{-}2\text{-Ph-}1,2,3,4\text{-}MnC_3B_7H_9]\ (\mathbf{1}^-) \quad (5)$$

As shown in Figures 6 and 7, the structures of both salts **1**$^{2-}$ and **1**$^-$ were crystallographically confirmed. The structural parameters of the decamethylcobalticinium cations are consistent with the previously reported structure.[44] There are no close contacts between the cations and the anions nor between **1**$^{2-}$ and the solvent molecule.

Wade[45] has predicted that 11-vertex *closo* geometries should be able to accommodate a wide variety of electron counts without undergoing a structural change, but it is clear that in both anions, **1**$^{2-}$ and **1**$^-$, cage opening has occurred. We have previously shown[11,15] that the tricarbadecaboranyl ligand in **1** can undergo an η^6 to η^4 cage-slippage upon the addition of a two-electron ligand. Thus, as shown in Figure 8, the cage-slipped η^4-coordinated complex 8-($CNBu^t$)-8,8,8-$(CO)_3$-9-Ph-*nido*-8,7,9,10-$MnC_3B_7H_9$, **3**, was formed in the addition reaction of **1** with *tert*-butyl isocyanide. This change in cage hapticity

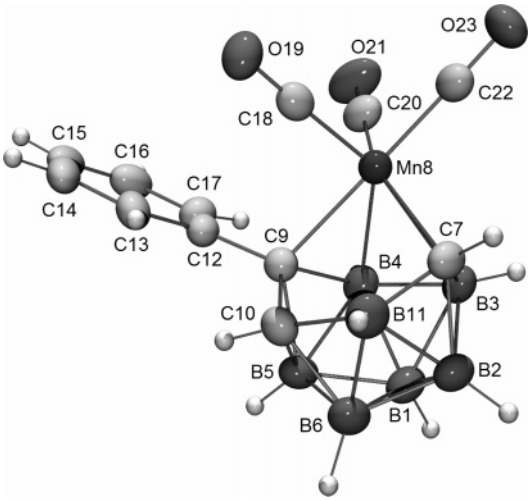

Figure 7. ORTEP representation of 8,8,8-$(CO)_3$-9-Ph-8,7,9,10-$MnC_3B_7H_9^{2-}$ (**1**$^-$). For selected distances see Table 3. Selected angles (deg): C7−Mn8−C9, 90.5(1); Mn8−C9−C12, 115.9(2); C9−Mn8−C18, 88.0(1); C9−Mn8−C20, 96.0(1); C9−Mn8−C22, 175.9(1); C7−Mn8−C18, 114.5(1); C7−Mn8−C20, 148.7(1); C7−Mn8−C22, 87.8(1); Mn8−C18−O19, 178.4(2); Mn8−C20−O21, 179.4(2); Mn8−C22−O23, 178.1(2).

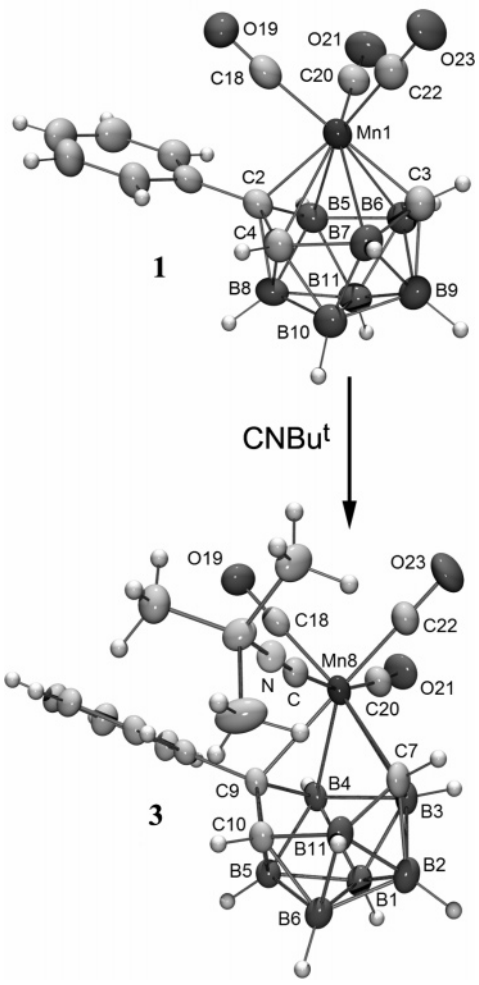

Figure 8. Reaction of 1,1,1-$(CO)_3$-2-Ph-*closo*-1,2,3,4-$MnC_3B_7H_9$, **1**, with *tert*-butyl isocyanide to form 8-($CNBu^t$)-8,8,8-$(CO)_3$-9-Ph-*nido*-8,7,9,10-$MnC_3B_7H_9$, **3** (ORTEPs are taken from ref 15).

reduces the electron donation of the tricarbadecaboranyl anion from 6 to 4 electrons, thus allowing the preservation of the 18-electron count of the metal. From a skeletal electron counting

(44) Braga, D.; Benedi, O.; Maini, L.; Grepioni, F. *J. Chem. Soc., Dalton Trans.* **1999**, 2611

(45) (a) O'Neill, M. E.; Wade, K. J. *J. Mol. Struct.* **1983**, *103*, 259. (b) Mulvey, R. E.; O'Neill, M. E.; Wade, K. J.; Snaith, R. *Polyhedron* **1986**, *5*, 1437. (c) O'Neill, M. E.; Wade, K. J. *Polyhedron* **1984**, *3*, 199.

Table 3. Selected Distances (Å)

	1[a]	**1**$^{2-}$	**1**$^{2-}$	**3**
Mn−C9	2.096(2) *Mn−C2*	2.153(2)	2.125(2)	2.267(2)
Mn−C7	2.049(3) *Mn−C3*	2.083(2)	2.138(2)	2.244(3)
Mn−C10	2.415(3) *Mn−C4*	2.911(3)	3.073(2)	3.135(2)
Mn−B4	2.346(3) *Mn−B5*	2.256(3)	2.157(2)	2.311(3)
Mn−B3	2.342(3) *Mn−B6*	2.269(3)	2.172(2)	2.340(3)
Mn−B11	2.408(3) *Mn−B7*	2.813(3)	3.100(2)	3.146(3)
C9−C10	1.508(3) *C2−C4*	1.523(3)	1.541(2)	1.518(3)
C10−B11	1.754(4) *C4−B7*	1.667(4)	1.611(3)	1.656(4)
C7−B11	1.576(4) *C3−B7*	1.585(4)	1.599(3)	1.586(4)
B3−C7	1.561(4) *C3−B6*	1.606(4)	1.648(3)	1.585(4)
B3−B4	1.885(4) *B5−B6*	1.834(4)	1.816(3)	1.923(5)
B4−C9	1.582(3) *C2−B5*	1.626(4)	1.676(2)	1.593(3)
Mn−C18	1.836(3)	1.812(2)	1.789(2)	1.838(3)
Mn−C20	1.792(3)	1.798(2)	1.783(2)	1.840(2)
Mn−C22	1.827(3)	1.805(2)	1.773(2)	1.832(3)
C18−O19	1.144(4)	1.153(3)	1.159(2)	1.142(4)
C20−O21	1.149(3)	1.150(3)	1.165(2)	1.138(3)
C22−O23	1.141(3)	1.156(3)	1.168(2)	1.137(4)

[a] Since **1** is a *closo* compound, it has a different numbering scheme (given in Figure 8 and in italics in the table) than **1**$^{2-}$, **1**$^{2-}$, and **3**.

Table 4. Selected DFT-Calculated Distances (Å) in Complexes 1m, 1m^{-}, and 1m^{2-}

	1m	**1m**$^{-}$	**1m**$^{2-}$
Mn−B3	2.323	2.273	2.205
Mn−B4	2.324	2.252	2.186
Mn−C9	2.164	2.199	2.159
Mn−C10	2.647	2.978	3.110
Mn−B11	2.445	2.894	3.148
Mn−C7	2.006	2.111	2.177
Mn−C	1.794−1.806	1.786−1.797	1.770−1.777
C−O	1.157−1.158	1.171−1.172	1.186−1.188

viewpoint, the addition of the two-electron isocyanide ligand increases the skeletal electron count of the manganatricarbadecaboranyl fragment to 26 skeletal electrons, and **3** therefore adopts an open-cage 11-vertex *nido* geometry based on an icosahedron missing one vertex.

The two-electron reduction of **1** produced the **1**$^{2-}$ dianion, which is isoelectronic with **3**. The crystallographic determination of **1**$^{2-}$ confirmed that it has a *nido* (i.e., slipped cage) geometry, analogous to that observed for **3**. In principle, the metal could slip to either the C7−B3−B4−C9 or the C9−C10−B11−C7 faces of the tricarbadecaboranyl cage. However, in agreement with the known preference of carbon atoms to adopt low-coordinate positions on the open face of clusters,[46] the slip occurs in both **1**$^{2-}$ and **3** such that the metals become η^4-coordinated to, and approximately centered over, the C7−B3−B4−C9 faces (Figures 6 and 8), thus producing five-membered, M−C7−B11−C10−C9, open faces containing all three cage carbons. From DFT calculations (see below) the isomer of **1** with Mn bound to C7−B3−B4−C9 is indeed more stable than the other isomer, with Mn bound to the opposite face, by 26 kcal mol^{-1}. The distances (Table 3) from Mn to C9, B4, B3, C7, C10, and B11 are similar but slightly longer in **3** (2.267(2), 2.311(3), 2.340(3), 2.243(3), 3.135(2), and 3.146(3) Å, respectively) than in **1**$^{2-}$ (2.125(2), 2.157(2), 2.172-(2), 2.138(2), 3.073(2), and 3.100(2) Å, respectively) with the dihedral angle between the C7−Mn8−C9 and the C9−C10−B11−C7 planes in **3** (150.7(1)°) being smaller than in **1**$^{2-}$ (156.7(1)°).

1^{-} contains only 25 skeletal electrons and, accordingly, adopts a structure (Figure 7) that is intermediate between the traditional 11-vertex *closo* (24 skeletal electrons) geometry observed for **1** and the *nido* (26 skeletal electons) geometry found for **3** and **1**$^{2-}$. Similar to **3** and **1**$^{2-}$, the tricarbadecaboranyl ligand in **1**$^{-}$ is slipped to an η^4 coordination and the manganese is closer to the center of the C7−B3−B4−C9 plane than the C9−C10−B11−C7 plane. The Mn−C10 and Mn−B11 distances (Table 3) in **1**$^{-}$ (2.911(3) and 2.813(3) Å) are between those of **1**$^{2-}$ (3.073(2) and 3.100(2) Å) and the analogous Mn−C4 and Mn−B7 distances in **1** (2.415(3) and 2.408(3) Å). The dihedral angle between the C7−Mn8−C9 and the C9−C10−B11−C7 planes (Figure 9) in **1**$^{-}$ (142.9(1)°) is also intermediate between those of **1**$^{2-}$ (156.7(1)°) and the equivalent C2−Mn1−C3/C2−C4−B7−C3 dihedral angle in **1** (117.6(1)°). The out-of-plane distance between Mn and the C2−C4−B7−C3 plane in **1** and the C9−C10−B11−C7 planes in **1**$^{-}$ and **1**$^{2-}$ decreases from 1.1352(3) Å in **1** to 0.8986(3) Å in **1**$^{-}$ and 0.6326(2) Å in **1**$^{2-}$, thus indicating an increase in planarity of the five-membered open face as electrons are added to the system.

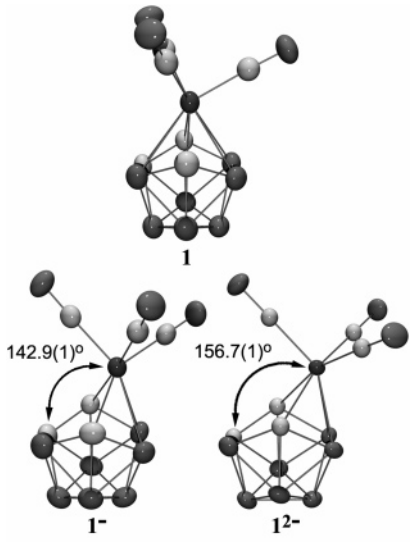

Figure 9. Comparisons of the dihedral angles between the C7−Mn8−C9 and the C9−C10−B11−C7 planes in **1**$^{-}$ (142.9(1)°) and **1**$^{2-}$ (156.7(1)°) and the equivalent C2−Mn1−C3/C2−C4−B7−C3 dihedral angle in **1** (117.6(1)°). Atom labels for **1**$^{2-}$, **1**$^{-}$, and **1** are given in Figures 6, 7, and 8, respectively.

In agreement with the IR data, discussed earlier, which indicate enhanced metal-to-CO back-bonding with increasing negative charge, the average Mn−C(carbonyl) distances shorten from 1.818(3) Å in **1** to 1.805(2) Å in **1**$^{-}$ and 1.782(2) Å in **1**$^{2-}$ (Table 3), while the average C−O distances lengthen from 1.145(3) Å in **1** to 1.153(3) Å in **1**$^{-}$ and 1.164(2) Å in **1**$^{2-}$. The average Mn−C(carbonyl) distance is larger (1.837(3) Å) and the average C−O distances is shorter (1.139(4) Å) in **3** compared to those in **1**$^{2-}$, indicating a reduced manganese to carbonyl π-bonding interaction in **3** that is consistent with competing manganese to isocyanide back-bonding.

III. Calculations and Electronic Character of Anions 1^{-} and 1^{2-}. DFT calculations[28] (ADF[29] program) were performed on models of the anions **1**$^{-}$ and **1**$^{2-}$, as well as the neutral parent complex and the monoanionic ligand, respectively **1m**$^{-}$, **1m**$^{2-}$, **1m**, and **L′**. The anionic *nido* [6-Me-5,6,9-$C_3B_7H_9$]$^{-}$ ligand presents a face with three carbon and three boron atoms to the metal and has therefore been considered as a Cp or a benzene analogue. However, the face is not planar and there are significant differences in the orbitals. Still, within the frontier orbitals (Figure 10), there are several orbitals with mainly π character, with the appropriate energy and symmetry to interact with the metal d levels.

(46) Williams, R. E. *Adv. Inorg. Chem. Radiochem.* **1976**, *18*, 67.

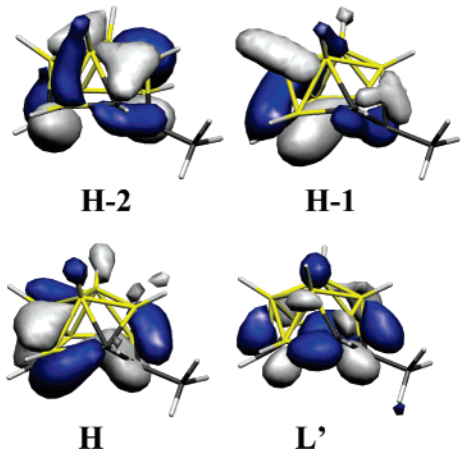

Figure 10. Frontier orbitals of [*nido*-6-Me-5,6,9-$C_3B_7H_9$]$^-$ (**L**).

The optimized geometries of the three complexes agree very well with those of the available X-ray structures, namely, the distances to the carborane face. The calculated Mn−C(O) and C−O distances, however, differ slightly more from the experimental ones, perhaps owing to the computational replacement of the phenyl group by a methyl group. In particular, it is interesting to analyze in detail the six Mn−C/B of the open face of the carborane, as well as the Mn−C(O) and C−O distances, as they give relevant information toward understanding the electronic changes accompanying reduction.

As was observed in the X-ray structures upon reduction, the Mn−C10 and Mn−B11 distances increase progressively (from 2.647 to 3.110 Å, and 2.445 to 3.148 Å, respectively), so that their length is no longer compatible with real bonds in the dianionic complex and is at a borderline situation in the monoanion. This behavior has been known as a ring-slippage or haptrotopic migration and studied computationally in detail for indenyl and cyclopentadienyl complexes.[16b,47]

Simultaneously, and in agreement with experimental data, the Mn−C7 distance also lengthens slightly, while the other three bonds shorten by an amount that is significant in terms of the error in the determination. In the reduction, therefore, the carborane goes from η^6 to η^4 hapticity. This behavior can be traced to the nature of the LUMO of the neutral complex **1m**, which is antibonding between Mn and the carborane face, as can be seen in Figure 11. It is delocalized over the Mn atom (32%), the carborane (30%), and the carbonyls (38%).

The Mn−C/B antibonding character is clearly seen in the LUMO of the neutral complex. Upon occupation, the distortion (moving two atoms away from the metal) leads to relief of this antibonding character and lowering of the energy of the new structure. The effect is reflected in the HOMO of the dianion **1m**$^{2-}$, where the repulsion is diminished by the larger distance (this is the same view as the one on the top left). This is exactly the mechanism operating in the ring-slippage reactions of indenyl, cyclopentadienyl, and other rings,[47] where the metal−ring antibonding character of the LUMO is relieved by haptotropic distortion. In the present carborane complex, the interaction between Mn and the two B atoms at the back (B3 and B4) also becomes bonding, resulting in the shortening of these bonds as electrons are added to the parent neutral complex.

Another important feature of the LUMO of **1m** (and indenyl complexes containing carbonyl ligands) is that back-donation makes it bonding between Mn and the carbonyl groups. Haptotropic shifts are usually favored in carbonyl complexes.[16b] Therefore, when the LUMO becomes occupied, the Mn−C(O) bond is expected to strengthen, while the C−O distance becomes longer. In the reduced anion, the haptotropic shift resulting in loss of one Mn−C and one Mn−B bond is compensated for by stronger metal bonding both to the carbonyls and to two borons of the carboranyl face. Combined, these changes lead to a significant charge redistribution within the molecule. Although Mulliken charges are not very reliable in terms of absolute values, they can be used to map trends in charge distribution. Along the series **1m** → **1m**$^-$ → **1m**$^{2-}$, the charge on the metal remains close to 0 (0.002 → 0.061 → 0.095). The boron atoms experience small changes, ranging between 0.123 and 0.424, 0.128 and 0.493, and 0.143 and 0.514, but becoming slightly more positive in general. Three of them have their positive charge increased by almost 0.1, though they stay within the previous range. A similar trend is observed for the carboranyl carbons (−0.139 to 0.058, −0.178 to 0.042, and −0.177 to 0.018, respectively), namely, small changes, becoming slightly more negative in this case. The charge goes to the carbonyls and the hydrogens attached to boron in the carborane. The negative charges of the latter increase by close to 0.15, while those of the carbon hydrogens barely change. In the carbonyls, both carbon and oxygen undergo significant changes in charge: while the positive charge of carbon drops from 0.415 to 0.450 in **1m**, to 0.328−0.344 in **1m**$^-$, and to 0.287−0.297 in **1m**$^{2-}$, that of oxygen becomes much more negative (ca. −0.407 in **1m**, ca. −0.476 in **1m**$^-$, ca. −0.549 in **1m**$^{2-}$). It is therefore clear that both the carbonyl and the carborane ligands play a role in absorbing the negative charges of the anions. As will be shown below in the Discussion, however, the dominant contribution to energetic stabilization of the anions comes from the η^6/η^4 hapticity change of the tricarbadecaboranyl ligand.

Finally, there exists the question of the spin-density distribution in the monoanion **1**$^-$, which, it will be recalled, could not be quantitatively derived from ESR measurements.

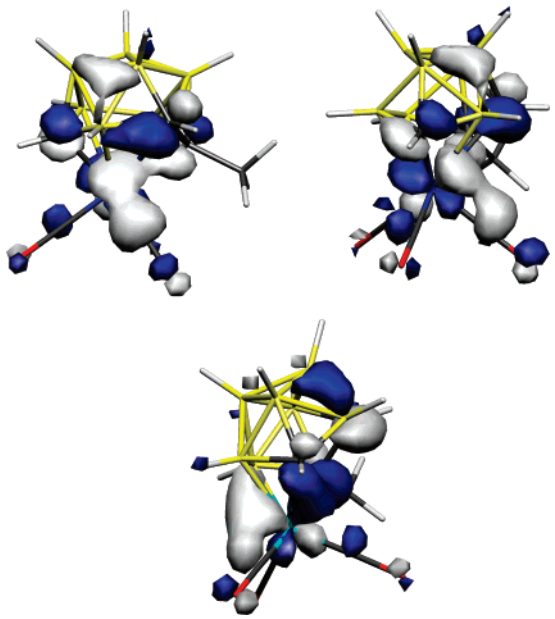

Figure 11. LUMO of 1,1,1-$(CO)_3$-2-Me-*closo*-1,2,3,4-$MnC_3B_7H_9$, **1m**, in two different views, depicting the Mn−C/B antibonding character (top) and the HOMO of the corresponding dianion **1m**$^{2-}$ (bottom), in Molekel representations (see Experimental Section).

(47) (a) Stoll, M. E.; Belanzoni, P.; Calhorda, M. J.; Drew, M. G. B.; Félix, V.; Geiger, W. E.; Gamelas, C. A.; Gonçalves, I. S.; Romão, C. C.; Veiros, L. F. *J. Am. Chem. Soc.* **2001**, *123*, 10595. (b) Calhorda, M. J.; Romão, C. C.; Veiros, L. F. *Chem.−Eur. J.* **2002**, *8*, 868.

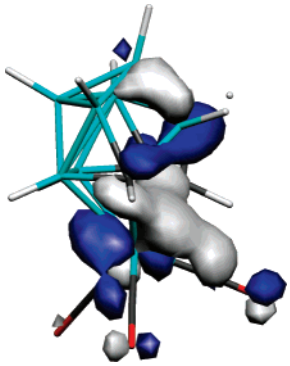

Figure 12. 3D representation of the SOMO of [1,1,1-$(CO)_3$-2-Me-*closo*-1,2,3,4-$MnC_3B_7H_9]^-$, **1m**$^-$.

Here, we point to the makeup of the SOMO derived for **1m**$^-$ to get an idea of the radical character of **1**$^-$. It is calculated to have 38% Mn character (up slightly from 32% in the LUMO of **1**, *vide ante*), 47% carborane character (vs 30% in **1**), and 15% total in the three carbonyls (down from 38% in **1**). Figure 12 gives a pictorial view of the SOMO of **1**$^-$. The major effect of the electron-transfer-induced hapticity change on the crucial valence orbitals is to increase the Mn(tricarbadecaboranyl) character at the expense of the carbonyl character.

IV. Single Two-Electron Reduction of 1,1,1-$(CO)_3$-2-Ph-*closo*-1,2,3,4-$ReC_3B_7H_9$, 2. Only a single two-electron quasi-reversible voltammogram was observed for the rhenium complex 1,1,1-$(CO)_3$-2-Ph-*closo*-1,2,3,4-$ReC_3B_7H_9$, **2**, showing that $E_{1/2}$ for the second reduction, **2**$^{-/2-}$, was never sufficiently negative of that for the first reduction, **2**$^{0/-}$, to allow voltammetric resolution of the two chemically reversible one-electron processes. In THF/[NBu_4][TFAB] an $E_{1/2}$ value of −1.30 V vs ferrocene was measured. The two-electron nature of the process **2**$^{0/2-}$ was confirmed by bulk cathodic electrolysis (E_{appl} = −1.45 V) at room temperature, which required exactly 2 F/equiv as the solution went from pale yellow to orange. Reverse anodic electrolysis (E_{appl} = −0.9 V) gave back about 60% of the original neutral compound, and several small byproduct waves were seen in the final solution.

Inspection of the voltammetric shapes of **2** was consistent with $E_{1/2}(1)$ being slightly *negative* of $E_{1/2}(2)$, i.e., "inverted" from normal behavior, as described by Evans.[37] A value of $\Delta E_{1/2}$ = −0.06 V was calculated both from the DPV width at half-height (66 mV) and the CV peak separation at slow sweep rates (iR_u-corrected value of 34 mV at 0.05 V s^{-1}).[48] The monoanion **2**$^-$ is thus seen to be thermodynamically unstable with respect to disproportionation (log K_{disp} = −log K_{comp} = 1.01).

Dramatic increases in ΔE_pwere noted at increased CV scan rates. This can be attributed to slow heterogeneous electron transfer in one or both of the one-electron redox processes **2**/**2**$^-$ and **2**$^-$/**2**$^{2-}$, suggesting that reduction of the neutral complex results in significant, and perhaps gradual, structural changes, as already seen for the Mn congener. The shapes of the waves were consistent with the second reduction being slower than the first,[49] but the lack of resolution of the two processes precluded confident determination of the individual charge-transfer rates. Nevertheless, digital simulations were carried out, and at least one reasonable set of fits had $E_{1/2}(1)$ = −1.33 V, $k_s(1)$ = 0.01 cm s^{-1}, $\alpha(1)$ = 0.40 and $E_{1/2}(2)$ = −1.27 V, $k_s(2)$ = 0.01 cm s^{-1}, $\alpha(2)$ = 0.70 (Figure 13). A diffusion coefficient of 4.5 × 10 $^{-6}$ cm^2 s^{-1} was obtained for **2** by chronoamperometry in THF/0.1 M [NBu_4][TFAB].

In order to estimate the positive shift of **2** compared to its cyclopentadienyl analogue $ReCp(CO)_3$, the reduction of which is apparently unreported, a CV experiment was performed on $ReCp(CO)_3$ in THF/0.5 M [NBu_4][$B(C_6F_5)_4$]. A single chemically irreversible cathodic wave was observed (E_p = −3.26 V vs FcH) of twice the height seen for the anodic peak of an identical concentration of ferrocene in the same solution. Although the differences in chemical reversibility (and, possibly, stoichiometry) for the reductions of the two Re compounds impose obvious limitations on comparison of their cathodic potentials, the measured values do fit well into the emerging picture. Using a potential of −3.2 V for $ReCp(CO)_3$ and −1.3 V for **2**, the tricarbadecaboranyl ligand is seen to facilitate the reduction by approximately 1.9 V, slightly greater than the 1.7 V observed for the Mn congener. In the only other available comparison of first- and second-row metal complexes (namely, those of Fe and Ru), the cathodic stabilization of the electron-rich derivative was also observed to be slightly greater for the heavier metal.[12b]

Chemical reduction of **2** in THF by 1 equiv of $CoCp^*_2$ gave an ESR signal of modest strength, having one broad asymmetric line at room temperature, g = 2.023, which disappeared after the solution was exposed to air. Although this spectrum is likely to arise from the monoanion **2**$^-$ present owing to its incomplete disproportionation, the lack of observable hyperfine splittings precludes the definitive assignment of the spectrum to **2**$^-$.

Discussion

The one-electron reduction of **1** ($E_{1/2}(1)$ = −1.14 V in THF) is an impressive 1.72 V positive of the reduction of cymantrene (−2.86 V in THF).[50] This potential difference compares quite well with the positive shifts previously reported for the reduction of tricarbadecaboranyl vs cyclopentadienyl full-sandwich iron complexes.[12b] At the heart of our inquiry was the question of why the tricarbadecaboranyl ligand induces such an astonishing stabilization of electron-rich metal complexes. Using the literature value of +0.44 V (compared to Cp) as the tricarbadecaboranyl ligand substituent effect,[12b] 1.28 V of the stabilization potential of the Mn monoanion complex is attributed to the η^6 to η^4 hapticity change that accompanies the one-electron reduction of **1**. Qualitatively similar reasoning accounts for the fact that the two one-electron potentials, $E_{1/2}(1)$ and $E_{1/2}(2)$, are so similar, their medium-dependent differences being much smaller than the values normally seen for successive redox reactions.[37,51] In this context, the significant further structural rearrangement with uptake of the second electron is seen as being responsible for an additional positive shift in $E_{1/2}(2)$. It is not possible to quantify the shift in $E_{1/2}(2)$ owing to the fact that the analogous cymantrene redox process, $[MnCp(CO)_3]^{-/2-}$, is unreported.

Not to be overlooked is the fact that both electron-transfer reactions of **1** display less than Nernstian charge-transfer kinetics. The measured k_s values of 8.8 × 10^{-3} and 2.0 × 10^{-2} cm s^{-1} for **1**/**1**$^-$ and **1**$^-$/**1**$^{2-}$, respectively, suggest that both

(48) The necessary analytical data are found in: Richardson, D. E.; Taube, H. *Inorg. Chem.* **1981**, *20*, 1278.

(49) (a) Ryan, M. D. *J. Electrochem. Soc.* **1978**, *125*, 547. (b) Bowyer, W. J.; Geiger, W. E. J. *Electroanal. Chem.* **1988**, *239*, 253.

(50) The reduction of cymantrene is chemically irreversible, so that the E_{pc} values reported in ref 10 are almost surely less negative than the correct $E_{1/2}$ value for $[MnCp(CO)_3]^{0/-}$. Although this difference is not likely to be large, we note that the potential shift that we calculate for replacement of Cp by tricarbadecaboranyl is, in fact, a lower limit.

(51) Separations of 500 mV or more are commonly observed for successive one-electron reductions of metal complexes. See, for example: (a) metal dithiolenes: ref 14a. (b) Metal carboranes: Callahan, K. P.; Hawthorne, M. F. *Adv. Organometal. Chem.* **1976**, *14*, 145.

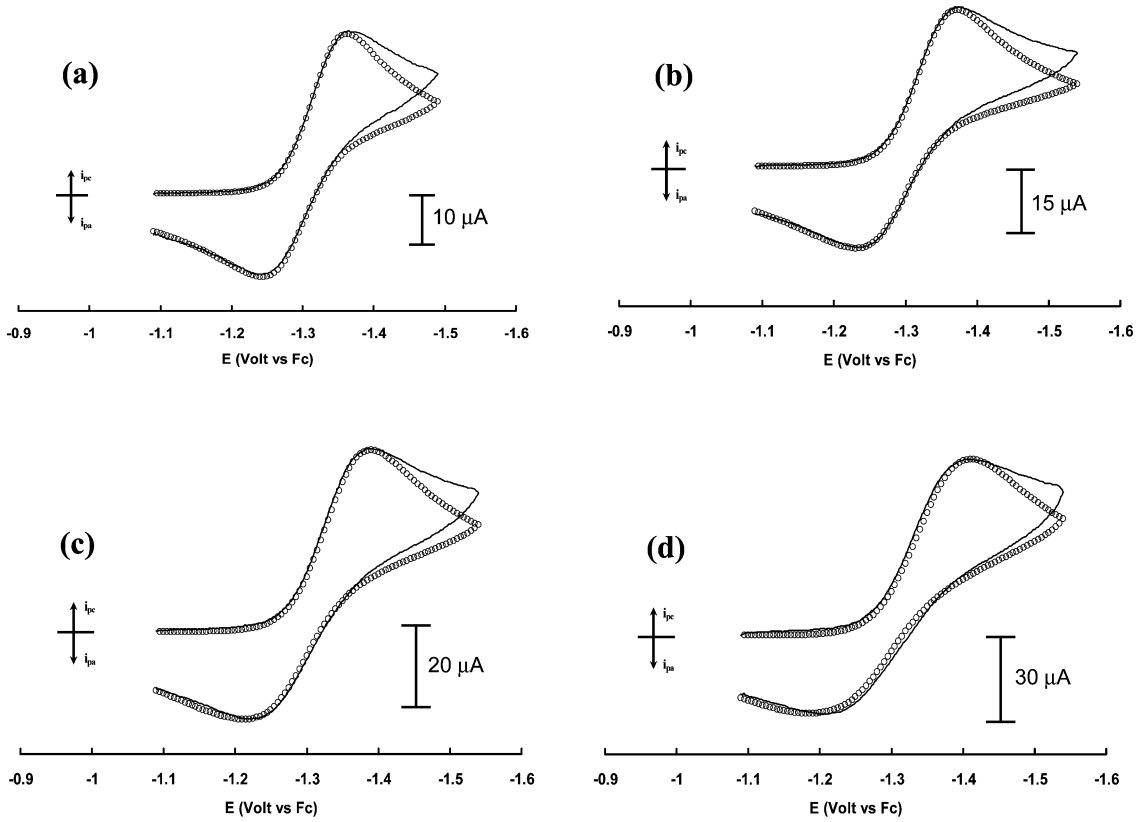

Figure 13. Experimental (solid) and simulated (circles) background-subtracted CV scans of 0.64 mM **2** in THF/0.1 M [NBu_4][TFAB] at 3 mm glassy carbon electrode and scan rates of (a) 0.3 V s^{-1} (b) 0.5 V s^{-1}, (c) 1.0 V s^{-1}, and (d) 2.0 V s^{-1}. See text for simulation parameters.

processes have a significant inner-sphere activation term, consistent with the structural changes being concomitant with electron transfer. The fact that the structural change on going from **1** to $\mathbf{1}^-$ is qualitatively half of that required to "complete" the transition to $\mathbf{1}^{2-}$ puts this complex into a small but increasing number of overall two-electron organometallic redox systems in which the one-electron intermediate is about midway in structure between the outlying members of the series.[47a,52]

Finally, the data compiled to date on the electrochemical properties of metal tricarbadecaboranyl complexes allow for some important generalizations to be made. When electrons are *removed* from tricarbadecaboranyl d^6 (e.g., Fe(II)) complexes, a simple ligand electronic effect operates to make the oxidation more difficult by about 0.44 V.[11,12] There is no evidence to date that significant structural changes accompany the d^6/d^5 redox processes. However, when electrons are *added* to these d^6 complexes, a lowering of the tricarbadecaboranyl hapticity occurs, thereby relieving the excess electron density at the metal. In terms of electron-counting, the monoanion $\mathbf{1}^-$ is neither an "18 + δ" complex (i.e., essentially a ligand-based radical)[53] nor a metal-based 19 e^- complex. Rather, it is very highly delocalized. Simple extreme models also fail to describe the dianion $\mathbf{1}^{2-}$. The tricarbadecaboranyl ligand has an enormous, arguably unprecedented, ability to accommodate low-valent metals by a combination of its electron-accepting properties and its hapto-sensitive structural flexibility.

Acknowledgment. We gratefully acknowledge support by NSF (CHE-0411703, Univ. Vermont, and CHE-0411682, Univ. Pennsylvania) and FCT (POCI/QUI/58925/2004, Lisbon).

Supporting Information Available: Figure S1 shows linear sweep voltammograms taken during the stepwise cathodic bulk electrolysis of **1**, first to $\mathbf{1}^-$ and then to $\mathbf{1}^{2-}$. Figure S2 shows square-wave voltammograms of **1**. This material is available free of charge via the Internet at http://pubs.acs.org.

OM700496V

(52) Westcott, S. A.; Kakkar, A. K.; Stringer, G.; Taylor, N. J.; Marder, T. B. *J. Organomet. Chem.* **1990**, *394*, 777.

(53) Tyler, D. R. *Acc. Chem. Res.* **1991**, *24*, 325.